THE LOCAL DISCONTINUOUS GALERKIN METHOD FOR CONVECTION-DIFFUSION-FRACTIONAL ANTI-DIFFUSION EQUATIONS

AFAF BOUHARGUANE * AND NOUR SELOULA &

Abstract. In this paper, we consider the discontinuous Galerkin method for solving time dependent partial differential equations with convection-diffusion terms and anti-diffusive fractional operator of order $\alpha \in (1,2)$. These equations are motivated by two distinct applications: a dune morphodynamics model and a signal filtering model. The key to study these numerical schemes is to split the anti-diffusive operators into a singular and non-singular integral representations. The problem is then expressed as a system of low order differential equations and a local discontinuous Galerkin method is proposed for these equations. We prove nonlinear stability estimates and optimal order of convergence $\mathcal{O}(\Delta x^{k+1})$ for linear equations and an order of convergence of $\mathcal{O}(\Delta x^{k+\frac{1}{2}})$ for the nonlinear problem. Finally numerical experiments are given to illustrate qualitative behaviors of solutions for both applications and to confirme our convergence results.

1. Introduction

In this paper, we are concerned with the numerical solutions for one-dimensional nonlocal scalar conservation law of the form:

$$\begin{cases} u_t + \left(f(u) - u_x + \mathcal{J}[u_x]\right)_x = 0, \quad x \in \mathbb{R}, \quad t > 0, \\ u(0,x) = u_0(x), \quad x \in \mathbb{R}, \end{cases} \tag{1.1}$$

where the unknown u depends on the space variable x and the time variable t. In (1.1), $f : \mathbb{R} \to \mathbb{R}$ is a continuous function, $\mathcal{J}$ is the anti-diffusive nonlocal operator and $u_0 : \mathbb{R} \to \mathbb{R}$ is the initial datum.
This kind of equation appears in the formation and dynamics of sand structures [17, 18] and they are also used as a filtering model [4]. They are given as follows.

2000 *Mathematics Subject Classification.* Primary 65M12, 65M60, 26A33 .
Key words and phrases. Convection-diffusion, Fractional anti-diffusion, Local discontinuous Galerkin methods, Stability, Convergence, Numerical simulations.
* Institut de Mathématiques de Bordeaux, CNRS UMR 5251; INRIA Bordeaux Sud-Ouest, France. E-mail: afaf.bouharguane@math.u-bordeaux.fr.
& Université de Caen, Laboratoire de Mathématiques Nicolas Oresme, CNRS UMR 6139, France. E-mail: nour-elhouda.seloula@unicaen.fr
This research was supported by the French National Center for Scientific Research (CNRS) through a young researcher PEPS project.

Dune morphodynamics model. In this case, we have $f(u) = u^2/2$ and the equation is given by

$$u_t + \left(\frac{u^2}{2} - u_x + \mathcal{J}^d[u_x]\right)_x = 0, \quad x \in \mathbb{R}, \quad t > 0, \tag{1.2}$$

where the nonlocal operator is defined as follows: for any Schwartz function $\varphi \in \mathcal{S}(\mathbb{R})$ and any $x \in \mathbb{R}$,

$$\mathcal{J}^d[\varphi](x) \quad := \quad \int_{-\infty}^{x} |x-\xi|^{-\frac{1}{3}} \varphi(\xi)\, d\xi. \tag{1.3}$$

The operator $\partial_x \mathcal{J}^d[u_x]$ can be seen as a fractional Laplacian of order $4/3$ since it has been proved that [3]

$$\mathcal{F}(\partial_x \mathcal{J}^d[u_x])(\xi) = -4\pi^2 \Gamma(\frac{2}{3}) \left(\frac{1}{2} - i\mathrm{sgn}(\xi)\frac{\sqrt{3}}{2}\right) |\xi|^{4/3} \mathcal{F}(u)(\xi),$$

where Γ is the gamma function and $\mathcal{F}$ denotes the Fourier transform.
This model appears in the work of Fowler [17] and describes the evolution of sand dunes in a river flow.

Signal filtering model. For this application $f = 0$ and the equation is given by

$$u_t - u_{xx} + \partial_x \mathcal{J}^s[u_x] = 0, \quad x \in \mathbb{R}, \quad t > 0, \tag{1.4}$$

where the nonlocal operator is a fractional Laplacian of order $\alpha \in (1, 2)$. Thanks to a Taylor-Poisson's formula and Fubini's theorem we can rewrite the nonlocal term as follows:

$$\mathcal{J}^s[\varphi](x) = C(\lambda) \int_{\mathbb{R}} |z|^{-\lambda} \varphi(x-z) dz \quad \text{with } \lambda = \alpha - 1 \in (0, 1) \tag{1.5}$$

This kind of equation has been proposed for signal filtering: it performs at the same time noise reduction (diffusion operator) and contrast enhancement (anti-diffusion operator) [4].

Note that in what follows, $\mathcal{J}$ refers both to the operators $\mathcal{J}^s$ and $\mathcal{J}^d$.

Equation (1.1) consists of three different terms: nonlinear convection $f(u)$, linear diffusion $-\partial_x^2 u$ and fractional anti-diffusive operator $\partial_x \mathcal{J}[u_x]$ .The main characteristic of these equations is the nonlocal operator which has a deregularizing effect on the initial data. Fortunately, these instabilities are controlled by the diffusion operator $-\partial_x^2 u$ which ensures the existence and the uniqueness of a smooth solution [3, 4]. We then always assume that there exists a sufficiently regular solution $u(t, x)$.

Besides the above cited, partial differential equations with nonlocal or fractional operators are widely used to model scientific problems in finance, mechanics, crow dynamics, traffic flow model ect. [6, 5, 22].
Therefore, several numerical methods have been suggested in the literature to overcome the difficulties faced by nonlocal equations. Droniou [16] used a general class of difference methods for fractional conservation laws, Zheng, Li and Zhao [32] proposed a finite element method to solve space-fractional advection equations. Deng [14] analyzed a finite element method for the numerical resolution of the space and

time fractional Fokker-Planck equation. Li, Huang and Wang [20] used a Galerkin finite element method and an implicit midpoint difference method to approximate the nonlinear fractional Ginzburg-Landau equation. Meerschaert and Tadjeran [23] studied finite difference approximations of fractional advection dispersion flow equation. Bueno-Orovio, Kay and Burrage [9] introduced Fourier spectral methods for fractional-in-space reaction-diffusion equations. Safari and Chen [25] proposed a coupling of the improved singular boundary method and dual reciprocity method for multi-term time-fractional mixed diffusion-wave equations. Recently Vong and Lyu [27] studied a second order finite difference schemes for spatial fractional differential equations with variable coefficients.

The Discontinuous Galerkin method (DG hereafter) is a finite element method which uses a completely discontinuous piecewise polynomial space for the numerical solution and the test functions. Advantages of DG methods are their higher order convergence property, their great flexibility in mesh construction, their easily handling of complex geometries, as well as its efficiency in parallel implementation. However, the main challenge in this method is based on the choice of the numerical flux which is essential to ensure the stability and accuracy of the scheme.

For the DG methods, recent works have been proposed to deal with equations involving fractional operators: Xu and Hesthaven [29] applied the local discontinuous Galerkin method to fractional convection diffusion equations with a fractional Laplacian of order $\alpha \in (1, 2)$. Mustapha and McLean [24] studied a discontinuous Galerkin method for fractional diffusion and wave equations. Cifani, Jakobsen and Karlsen [10] studied fractional degenerate convection-diffusion equation ($\alpha \in (0, 1)$) and, Deng and Hesthaven [15] a local discontinuous Galerkin method for fractional diffusion equations. Cockburn and Mustapha [13] investigated a hybridizable discontinuous Galerkin method for fractional diffusion problems. Aboelenen and El-Hawary [1] developed a nodal discontinuous Galerkin method for the linearized fractional Cahn-Hillard equation. Recently, Ahmadinia, Safari and Fouladi [2] analyzed a local discontinuous Galerkin method for time-space fractional convection-diffusion equations.

For equations like (1.1), few numerical methods have been developed up to now: finite difference method [3], split-step Fourier method [7] and finite element method [8] have been used to perform numerical simulations for the Fowler equation (1.2). More recently [19] proposed finite difference schemes for fractional water waves models.
We propose in this paper to develop a DG method for equations (1.1). We consider in particular the Local Discontinuous Galerkin (LDG hereafter) since the equations contain higher order spatial derivatives. The idea of LDG methods is to rewrite the equation into a first order system and then apply the discontinuous Galerkin method to the system [11].
The application of the LDG method to the convection-diffusion-fractional anti-diffusion equations allows to get a numerical scheme of order $O(\Delta x^{k+1})$ (resp. $O(\Delta x^{k+1/2})$) for linear (resp. nonlinear) case. A similar convergence result has been obtained using only finite element method in [8]. But the advantages of this method reside on the specificity of the DG methods like their local nature.

In comparison with the results presented in [29] the main difference in this paper resides on the way to control the anti-diffusive effects of the nonlocal operators. For that, we decompose the fractional operators into a singular and non-singular integrals. As a consequence, a part of the anti-diffusive fractional operator is controlled with the diffusion term.

To control the fractional operator with the diffusion term, we write the nonlocal terms as follows:
Let r be a strictly positive constant such that

Dune model Integrating by parts we can rewrite $\mathcal{J}^d$ as

$$\mathcal{J}^d[\varphi'](x) := \mathcal{J}_1^d[\varphi'](x) + \mathcal{J}_2^d[\varphi](x), \tag{1.6}$$

where

$$\mathcal{J}_1^d[\varphi](x) = \int_{x-r}^{x} |x-\xi|^{-1/3}\varphi(\xi)\,d\xi$$

and

$$\mathcal{J}_2^d[\varphi](x) = -\frac{1}{3}\int_{-\infty}^{x-r} |x-\xi|^{-4/3}\varphi(\xi)\,d\xi + r^{-1/3}\varphi(x-r).$$

Signal model: As previously by integrating by parts and since φ is a Schwartz function, we rewrite $\mathcal{J}^s$ as

$$\begin{aligned}
\mathcal{J}^s[\varphi'](x) &= C(\lambda)\int_{-\infty}^{-r} |\xi|^{-\lambda}\varphi'(x-\xi)\,d\xi + C(\lambda)\int_{-r}^{r} |\xi|^{-\lambda}\varphi'(x-\xi)\,d\xi \\
&+ C(\lambda)\int_{r}^{\infty} |\xi|^{-\lambda}\varphi'(x-\xi)\,d\xi \\
&= C(\lambda)\int_{|\xi|<r} |\xi|^{-\lambda}\varphi'(x-\xi)\,d\xi + C(\lambda)\left(\lambda\int_{-\infty}^{-r} |\xi|^{-\lambda-1}\varphi(x-\xi)\,d\xi - r^{-\lambda}\varphi(x+r)\right) \\
&+ C(\lambda)\left(-\lambda\int_{r}^{\infty} |\xi|^{-\lambda-1}\varphi(x-\xi)\,d\xi + r^{-\lambda}\varphi(x-r)\right)
\end{aligned}$$

Therefore, we decompose $\mathcal{J}^s$ as

$$\mathcal{J}^s[\varphi'](x) := \mathcal{J}_1^s[\varphi'](x) + \mathcal{J}_2^s[\varphi](x), \tag{1.7}$$

where

$$\mathcal{J}_1^s[\varphi](x) = C(\lambda)\int_{|\xi|<r} |\xi|^{-\lambda}\varphi(x-\xi)\,d\xi$$

and

$$\begin{aligned}
\mathcal{J}_2^s[\varphi](x) &= C(\lambda)\lambda\left(-\int_{r}^{\infty} |\xi|^{-\lambda-1}\varphi(x-\xi)\,d\xi + \int_{-\infty}^{-r} |\xi|^{-\lambda-1}\varphi(x-\xi)\,d\xi\right) \\
&+ C(\lambda)\left(r^{-\lambda}\varphi(x-r) - r^{-\lambda}\varphi(x+r)\right).
\end{aligned}$$

This splitting helps to control the nonlocal term with the diffusion operator: indeed we prove for r well chosen that the operator $\mathcal{J}_1$ is completely controlled with the diffusion operator. Note that the operator $\mathcal{J}_2$ does not need to be controlled because this term will be bounded by the L^2 norm of the solution, which is a natural

behavior because solutions of these equations are stable in the sense of (3.1).

The rest of this paper is organized as follows. In the next section, we introduce the semi-discrete LDG method for equations (1.2) and (1.4) and we prove some useful results. In sections 3 and 4, we prove that both approximations are L^2 stable and optimal order of convergence $\mathcal{O}(\Delta x^{k+1})$ for linear equations and an order of convergence of $\mathcal{O}(\Delta x^{k+\frac{1}{2}})$ for the nonlinear problem. Finally in section 5, we present numerical experiments to illustrate both applications and we validate the convergence results stated in the previous section.

2. The semi-discrete LDG method

For numerical simulations, it is more convenient to restrict the problem to a domain $\Omega = (-1, 1) \subset \mathbb{R}$. Therefore, we impose homogeneous Dirichlet boundary conditions in $\mathbb{R}\backslash\Omega$.
We then choose a partition of Ω consisting of cells $I_j = (x_j, x_{j+1})$, $j = 0, \ldots, M$ where $-1 = x_0 < x_1 < \cdots < x_M < x_{M+1} = 1$. We denote the cell lengths $\Delta x_j = x_{j+1} - x_j$ and we define $\Delta x = \max\limits_{j=1,\cdots,M} \Delta x_j$.

We denote by $P^k(I_j)$ the space of all polynomials of degree at most k with support on I_j, and we define the piecewise polynomial space V^k as

$$V^k = \left\{ v \,;\, v_{|I_j} \in P^k(I_j), j = 0, \cdots, M \right\}.$$

Let us finally introduce the operators

$$[v]_j = v(x_j^+) - v(x_j^-), \quad \overline{v(x_j)} = \frac{1}{2}(v(x_j^+) + v(x_j^-)).$$

where

$$v(x_j^\pm) = \lim_{x \to x_j^\pm} v(x).$$

2.1. Formulation of the LDG scheme .

Let us introduce the numerical schemes for the dune morphodynamics model (1.2) and the signal filtering model (1.4). Taking into account the decomposition (1.6) and (1.7), we introduce two variables v, q, and set

$$\begin{aligned} q &= -v + \mathcal{J}_1[v] + \mathcal{J}_2[u] \\ v &= \frac{\partial u}{\partial x}. \end{aligned}$$

Signal model. In this case, the linear problem is rewritten as follows

$$\begin{cases} \frac{\partial u}{\partial t} + \frac{\partial q}{\partial x} = 0 \\ q = -v + \mathcal{J}_1^s[v] + \mathcal{J}_2^s[u] \\ v = \frac{\partial u}{\partial x} \end{cases}$$

Dune model.

The nonlinear problem can be rewritten as

$$\begin{cases} \frac{\partial u}{\partial t} + \frac{\partial}{\partial x} f(u) + \frac{\partial q}{\partial x} = 0 \\ q = -v + \mathcal{J}_1^d[v] + \mathcal{J}_2^d[u] \\ v = \frac{\partial u}{\partial x} \end{cases}$$

In both cases, we seek an approximation $(u_h, q_h, v_h) \in V^k \times V^k \times V^k$ to (u, q, v) such that, for any $\varphi_u, \varphi_q, \varphi_v \in V^k$, we have

Signal model.

$$(2.1) \quad \begin{cases} (\frac{\partial u_h}{\partial t}, \varphi_u)_{I_j} - (q_h, \varphi_u')_{I_j} + \widehat{q_h}\, \varphi_u|_{x_j^+}^{x_{j+1}^-} = 0 \\ (q_h, \varphi_q)_{I_j} = -(v_h, \varphi_q)_{I_j} + (\mathcal{J}_1^s[v_h], \varphi_q)_{I_j} + (\mathcal{J}_2^s[u_h], \varphi_q)_{I_j} \\ (v_h, \varphi_v)_{I_j} = -(u_h, \varphi_v')_{I_j} + \widehat{u_h}\varphi_v|_{x_j^+}^{x_{j+1}^-} \\ (u_h(0,\cdot), \varphi_v)_{I_j} - (u_0, \varphi_v)_{I_j} = 0 \end{cases}$$

Dune model.

$$(2.2) \quad \begin{cases} (\frac{\partial u_h}{\partial t}, \varphi_u)_{I_j} - (f(u_h) + q_h, \varphi_u')_{I_j} + \left(\hat{f}_h\varphi_u + \hat{q}_h\, \varphi_u\right)|_{x_j^+}^{x_{j+1}^-} = 0 \\ (q_h, \varphi_q)_{I_j} = -(v_h, \varphi_q)_{I_j} + (\mathcal{J}_1^d[v_h], \varphi_q)_{I_j} + (\mathcal{J}_2^d[u_h], \varphi_q)_{I_j} \\ (v_h, \varphi_v)_{I_j} = -(u_h, \varphi_v')_{I_j} + \hat{u}_h\varphi_v|_{x_j^+}^{x_{j+1}^-} \\ (u_h(0,\cdot), \varphi_v)_{I_j} - (u_0, \varphi_v)_{I_j} = 0 \end{cases}$$

To complete the LDG schemes (2.1) and (2.2), we now introduce the numerical fluxes.
For the high order derivative part, it is well know that a good choice to guarantee the stability and solvability is to consider the following numerical fluxes [11, 30]

$$\widehat{u_h}_j = u_h(x_j^-), \quad \widehat{q_h}_j = q_h(x_j^+). \tag{2.3}$$

or

$$\widehat{u_h}_j = u_h(x_j^+), \quad \widehat{q_h}_j = q_h(x_j^-). \tag{2.4}$$

At the external boundaries we use

$$\widehat{q}_h(t,-1) = q_h^+(t,-1) = q_h^-(t,-1); \quad \widehat{q}_h(t,1) = q_h^+(t,1) = q_h^-(t,1); \tag{2.5}$$

and

$$\widehat{u}_h(t,-1) = 0; \quad \widehat{u}_h(t,1) = 0. \tag{2.6}$$

For the nonlinear part $\hat{f}_h$, any consistent (i.e. $\widehat{f}_h(u,u) = f(u)$) and monotone (i.e. increasing w.r.t. its first variable and decreasing w.r.t. its second variable) numerical flux can be used [12]

$$\widehat{f}_h(u_j) = \widehat{f}(u(x_j^-), u(x_j^+)).$$

2.2. **Some useful results.**

Lemma 2.1. *The following result holds for any $v \in V^k$*

1. *Dune model:*
   a. $||\mathcal{J}_1^d[v]||^2_{L^2(\Omega)} \leq C(r^{1/3})\,||v||^2_{L^2(\Omega)}$
   b. $||\mathcal{J}_2^d[v]||^2_{L^2(\Omega)} \leq c(1+r^{-2/3})\,||v||^2_{L^2(\Omega)}$
2. *Signal model :*
   a. $||\mathcal{J}_1^s[v]||^2_{L^2(\Omega)} \leq C(r^{\lambda})\,||v||^2_{L^2(\Omega)}, \quad \forall \lambda \in (0,1/2)$
   b. $||\mathcal{J}_1^s[v]||^2_{L^2(\Omega)} \leq C(r^{2(1-\lambda)})\,||v||^2_{L^2(\Omega)}, \quad \forall \lambda \in (1/2,1)$
   c. $||\mathcal{J}_2^s[v]\,||^2_{L^2(\Omega)} \leq C(r^{-2\lambda})\,||v||^2_{L^2(\Omega)}, \quad \forall \lambda \in (0,1)$

Proof. 1. Let us study the operators $\mathcal{J}_1^d$ and $\mathcal{J}_2^d$ associated to the dune morphodynamics equation (1.2).

a. Using Cauchy-Schwarz's inequality, we obtain for all $x \in \Omega$

$$\begin{aligned} |\mathcal{J}_1^d[v](x)|^2 &\leq \left(\int_{x-r}^{x} |x-\xi|^{-2/3} d\xi\right) ||v||^2_{L^2(\Omega)} \\ &\leq 3r^{1/3}||v||^2_{L^2(\Omega)} \end{aligned}$$

and by integrating over Ω we obtain

$$\int_\Omega |\mathcal{J}_1^d[v](x)|^2 \leq 6r^{1/3}||v||^2_{L^2(\Omega)}.$$

b. Using the equivalence of norms in finite dimensional spaces, we obtain

$$|\mathcal{J}_2^d[v](x)| \leq C\left(r^{-1/3} - (x+1)^{-1/3}\right)||v||_{L^2(\Omega)} + Cr^{-1/3}||v||_{L^2(\Omega)}.$$

Therefore, we have

$$|\mathcal{J}_2^d[v](x)|^2 \leq C\left(r^{-2/3} + (x+1)^{-2/3}\right)||v||^2_{L^2(\Omega)}.$$

By integrating, we get

$$\int_\Omega |\mathcal{J}_2^d[v](x)|^2\,dx \leq c(r^{-2/3}+1)||v||^2_{L^2(\Omega)}.$$

2. For $\lambda \in (0,1/2)$, the proof for the operators $\mathcal{J}_1^s$ and $\mathcal{J}_2^s$ is similar to the previous ones.
For $\lambda \in (1/2,1)$, we use again the equivalence of norms in finite dimensional spaces to get the result.

□

Remark 2.2. Note that if $x \pm r$ is a node of the mesh, nothing change for the term $\mathcal{J}_1$ but we have to be careful for $\mathcal{J}_2$. Indeed, for example, $\mathcal{J}_2^d$ can be approximated by:

$$\mathcal{J}_2^d[v](x) = -\frac{1}{3}\int_{-\infty}^{x_{k^*}} |x-\xi|^{-4/3} v(\xi)\,d\xi + r^{-1/3} v(x_{k^*}^-),$$

where $x_{k^*} = x - r$. Therefore, using again Young's inequality and inverse inequality, we obtain exactly the same estimate proved in Lemma 2.1 where we have assumed that $x - r$ is not a node.
As a consequence, in the remainder of this work, we will not make the difference if $x \pm r$ is a node of the mesh or not.

Lemma 2.3 (Gronwall lemma [26]). *Let $y(t), h(t), g(t), f(t)$ be nonnegative functions such that $\int_0^T g(t)\,dt \leq M$ and either*

$$y(t) + \int_0^t h(s)\,ds \leq y(0) + \int_0^t (g(s)y(s) + f(s))\,ds, \quad \forall 0 \leq t \leq T,$$

or

$$\frac{d}{dt}y(t) + h(t) \leq g(t)y(t) + f(t), \quad \forall 0 \leq t \leq T.$$

Then

$$y(t) + \int_0^t h(s)\,ds \leq e^M \left(y(0) + \int_0^t f(s)\,ds \right), \quad \forall 0 \leq t \leq T.$$

3. The linear and nonlinear stability

Let us first review the stability property for the continuous problem. Let $u \in C((0,T), L^2(\Omega))$ be a smooth solution to the initial value problem (1.2) or (1.4). Then, we can prove using Fourier analysis that (see [8] for (1.2) and [4] for (1.4))

$$||u(t,\cdot)||_{L^2(\Omega)} \leq e^{w_* t}||u_0||_{L^2(\Omega)}, \quad \forall t \in (0,T) \tag{3.1}$$

where w_* is a positive constant.
Therefore, we say that the LDG schemes (2.1) and (2.2) are L^2-stable if the numerical solutions u_h satisfy

$$||u_h(T,\cdot)||_{L^2(\Omega)} \leq C(T)||u_0||_{L^2(\Omega)}.$$

The goal of this section is then to prove the numerical stability of the LDG schemes (2.1) and (2.2). For that, let us some over all j, add the three equations, integrate over $t \in (0,T)$ and define two functionals associated to both models (2.1) and (2.2):

Signal model.

$$\begin{aligned}
&\mathcal{B}^s(u_h, q_h, v_h; \varphi_u, \varphi_q, \varphi_v) \\
&= \int_0^T ((u_h)_t, \varphi_u)\,dt - \int_0^T \sum_{j=0}^{M} (q_h, \varphi_u')_{I_j}\,dt - \int_0^T \sum_{j=1}^{M} (\hat{q}_h)_j\,[\varphi_u]_j dt \\
&- \int_0^T (q_h^+(t,-1)\varphi_u^+(-1) - q_h^-(t,1)\varphi_u^-(1))\,dt + \int_0^T (q_h, \varphi_q)\,dt + \int_0^T (v_h, \varphi_q)\,dt \\
&- \int_0^T (\mathcal{J}_1^s[v_h], \varphi_q)\,dt - \int_0^T (\mathcal{J}_2^s[u_h], \varphi_q)\,dt + \int_0^T (v_h, \varphi_v)\,dt \\
&+ \int_0^T \sum_{j=0}^{M} (u_h, \varphi_v')_{I_j}\,dt + \int_0^T \sum_{j=0}^{M} (\widehat{u}_h)_j [\varphi_v]_j\,dt
\end{aligned} \tag{3.2}$$

(3.3)

Dune model.

We first define the functional associated to the linear part

$$\begin{aligned}\mathcal{B}_l^d(u_h,q_h,v_h;\varphi_u,\varphi_q,\varphi_v) &= \int_0^T ((u_h)_t,\varphi_u)\,dt - \int_0^T \sum_{j=0}^{M}(q_h,\varphi_u')_{I_j}dt - \int_0^T \sum_{j=1}^{M}(\hat{q}_h)_j\,[\varphi_u]_j dt\\ &- \int_0^T (q_h^+(t,-1)\varphi_u^+(-1) - q_h^-(t,1)\varphi_u^-(1))\,dt + \int_0^T (q_h,\varphi_q)\,dt + \int_0^T (v_h,\varphi_q)\,dt\\ &- \int_0^T (\mathcal{J}_1^d[v_h],\varphi_q)\,dt - \int_0^T (\mathcal{J}_2^d[u_h],\varphi_q)\,dt + \int_0^T (v_h,\varphi_v)\,dt\\ &+ \int_0^T \sum_{j=0}^{M}(u_h,\varphi_v')_{I_j}\,dt + \int_0^T \sum_{j=0}^{M}(\widehat{u}_h)_j[\varphi_v]_j\,dt\end{aligned} \tag{3.4}$$

then the functional associated to the dune model (2.2) is given by

$$\begin{aligned}\mathcal{B}^d(u_h,q_h,v_h;\varphi_u,\varphi_q,\varphi_v) &= \mathcal{B}_l^d(u_h,q_h,v_h;\varphi_u,\varphi_q,\varphi_v)\\ &- \int_0^T \sum_{j=0}^{M}(f(u_h),\varphi_u')_{I_j}dt - \int_0^T \sum_{j=0}^{M}\hat{f}_h[\varphi_u])_j dt\end{aligned} \tag{3.5}$$

because $f(0)=0$.

Lemma 3.1. *For any $u,v,q\in V^k$, the following result holds*

(1) *Signal Model.*

$$\begin{aligned}\mathcal{B}^s(u,q,v;u,v,-q) &= \frac{1}{2}||u(T,\cdot)||^2_{L^2(\Omega)} - \frac{1}{2}||u_0||^2_{L^2(\Omega)} + \int_0^T ||v(t,\cdot)||^2_{L^2(\Omega)}dt\\ &\quad - \int_0^T (\mathcal{J}_1^s[v],v)\,dt - \int_0^T (\mathcal{J}_2^s[u],v)\,dt\end{aligned}$$

(2) *Dune Model.*

$$\begin{aligned}\mathcal{B}^d(u,q,v;u,v,-q) &= \frac{1}{2}||u(T,\cdot)||^2_{L^2(\Omega)} - \frac{1}{2}||u_0||^2_{L^2(\Omega)} + \int_0^T ||v(t,\cdot)||^2_{L^2(\Omega)}dt\\ &- \int_0^T (\mathcal{J}_1^d[v],v)\,dt - \int_0^T (\mathcal{J}_2^d[u],v)\,dt + \int_0^T \sum_{j=0}^{M}\Big([\Phi(u)]_j - (\hat{f}_h[u])_j\Big)\,dt\end{aligned}$$

where $\Phi(u)=\int^u f(u)\,du$.

Proof. (1) Signal Model

We set $(\varphi_u,\varphi_q,\varphi_v)=(u,v,-q)$ in (3.3) and we obtain

$$\begin{aligned}\mathcal{B}^s(u,q,v;u,v,-q) &= \frac{1}{2}||u(T,\cdot)||^2_{L^2(\Omega)} - \frac{1}{2}||u_0||^2_{L^2(\Omega)} + \int_0^T ||v(t,\cdot)||^2_{L^2(\Omega)}\\ &- \int_0^T (\mathcal{J}_1^s[v],v)\,dt - \int_0^T (\mathcal{J}_2^s[u],v) - (q^+(t,-1)u^+(t,-1) - q^-(t,1)u^-(t,1))\,dt\\ &- \int_0^T \sum_{j=0}^{M}\big((q,u_x)_{I_j} + (u,q_x)_{I_j}\big)\,dt - \int_0^T \sum_{j=1}^{M}(\hat{q}_j[u]_j + \hat{u}_j[q]_j)\,dt\end{aligned}$$

Using the integration by parts $(q,u_x)_{I_j}+(u,q_x)_{I_j}=(u\,q)|_{x_j^+}^{x_{j+1}^-}$, the numerical fluxes (2.3) or (2.4) with the external boundaries (2.5) and (2.6) we obtain

$$\begin{aligned}-\sum_{j=0}^{M}\big((q,u_x)_{I_j}+(u,q_x)_{I_j}\big) &= \sum_{j=1}^{M}[u\,q]_j+q^+(t,-1)u^+(t,-1)-q^-(t,1)u^-(t,1)\\ &= \sum_{j=1}^{M}(\hat{q}_j[u]_j+\hat{u}_j[q]_j)+q^+(t,-1)u^+(t,-1)-q^-(t,1)u^-(t,1)\end{aligned}$$

(2) Dune Model
As previously, we set $(\varphi_u,\varphi_q,\varphi_v)=(u,v,-q)$ in (3.5), and using the numerical fluxes defined in (2.3) or (2.4) we have

$$\begin{aligned}\mathcal{B}^d(u,q,v;u,v,-q) &= \frac{1}{2}||u(T,\cdot)||^2_{L^2(\Omega)}-\frac{1}{2}||u_0||^2_{L^2(\Omega)}+\int_0^T||v(t,\cdot)||^2_{L^2(\Omega)}dt\\ &- \int_0^T\sum_{j=0}^{M}(f(u),u_x)_{I_j}dt-\int_0^T\sum_{j=1}^{M}(\hat{f}_h[u])_j dt\\ &- \int_0^T(\mathcal{J}_1^d[v],v)_{I_j}\,dt-\int_0^T(\mathcal{J}_2^d[u],v)_{I_j}\,dt\end{aligned}$$

and since $f(0)=0$ we get

$$\int_0^T\sum_{j=0}^{M}(f(u),u_x)_{I_j}dt=-\int_0^T\sum_{j=1}^{M}[\Phi(u)]_j dt$$

then we obtain

$$\begin{aligned}\mathcal{B}^d(u,q,v;u,v,-q) &= \frac{1}{2}||u(T,\cdot)||^2_{L^2(\Omega)}-\frac{1}{2}||u_0||^2_{L^2(\Omega)}+\int_0^T||v(t,\cdot)||^2_{L^2(\Omega)}dt\\ &- \int_0^T(\mathcal{J}_1^d[v],v)\,dt-\int_0^T(\mathcal{J}_2^d[u],v)\,dt+\int_0^T\sum_{j=1}^{M}\Big([\Phi(u)]_j-(\hat{f}_h[u])_j\Big)\,dt\end{aligned}$$

which concludes the proof of this Lemma.

□

Theorem 3.2 (Linear stability)**.** *The LDG scheme* (2.1) *is L^2-stable, and its solution satisfies*

$$||u_h(T,\cdot)||^2_{L^2(\Omega)}+\int_0^T||v_h(t,\cdot)||^2_{L^2(\Omega}\,dt\le C(\lambda,T)||u_0||^2_{L^2(\Omega)}$$

Proof. Without loss of generality we assume $\lambda\in(0,1/2)$.
By construction and thanks to (2.1) we have $\mathcal{B}^s(u_h,q_h,v_h;\varphi_u,\varphi_q,\varphi_v)=0$ for all $\varphi_u,\varphi_q,\varphi_v\in V^k$.
Then, we have for $(\varphi_u,\varphi_q,\varphi_v)=(u_h,v_h,-q_h)$,

$$\mathcal{B}^s(u_h,q_h,v_h;u_h,v_h,-q_h)=0$$

From Lemma 3.1, Lemma 2.1 and Hölder's inequality, we obtain

$$\begin{aligned}
&\frac{1}{2}||u_h(T,\cdot)||^2_{L^2(\Omega)} - \frac{1}{2}||u_0||^2_{L^2(\Omega)} + \int_0^T ||v_h(t,\cdot)||^2_{L^2(\Omega)}\,dt \\
&\leq \int_0^T ||\mathcal{J}_1^s[v_h(t,\cdot)]||_{L^2(\Omega)}||v_h(t,\cdot)||_{L^2(\Omega)}\,dt + \int_0^T ||\mathcal{J}_2^s[u_h(t,\cdot)]||_{L^2(\Omega)}||v_h(t,\cdot)||_{L^2(\Omega)}\,dt \\
&\leq C(r^{\frac{\lambda}{2}}) \int_0^T ||v_h(t,\cdot)||^2_{L^2(\Omega)}\,dt + \int_0^T ||\mathcal{J}_2^s[u_h(t,\cdot)]||^2_{L^2(\Omega)}\,dt + \frac{1}{4}\int_0^T ||v_h(t,\cdot)||^2_{L^2(\Omega)}\,dt \\
&\leq \left(C(r^{\frac{\lambda}{2}}) + \frac{1}{4}\right) \int_0^T ||v_h(t,\cdot)||^2_{L^2(\Omega)}\,dt + C(r^{-\lambda}) \int_0^T ||u_h(t,\cdot)||^2_{L^2(\Omega)}\,dt
\end{aligned}$$

we then choose r such that $C(r^{\frac{\lambda}{2}}) + \frac{1}{4} = \frac{1}{2}$ and we obtain

$$\frac{1}{2}||u_h(T,\cdot)||^2_{L^2(\Omega)} - \frac{1}{2}||u_0||^2_{L^2(\Omega)} + \frac{1}{2}\int_0^T ||v_h(t,\cdot)||^2_{L^2(\Omega)}\,dt \leq C(\lambda)\int_0^T ||u_h(t,\cdot)||^2_{L^2(\Omega)}\,dt$$

Finally, using Gronwall's lemma (see Lemma 2.3) with

$$y(t) = ||u_h(t,\cdot)||^2_{L^2(\Omega)}, h(t) = ||v_h(t,\cdot)||^2_{L^2(\Omega)}, g(t) = C(\lambda) \text{ and } f(t) = 0,$$

we obtain the following result

$$\left\{||u_h(T,\cdot)||^2_{L^2(\Omega)} + \int_0^T ||v_h(t,\cdot)||^2_{L^2(\Omega)}dt\right\}^{1/2} \leq ||u_0||_{L^2(\Omega)}e^{C(\lambda)T}.$$

□

Theorem 3.3 (Nonlinear stability)**.** *The LDG scheme* (2.2) *is L^2-stable, and their solution satisfies*

$$||u_h(T,\cdot)||^2_{L^2(\Omega)} + \int_0^T ||v_h(t,\cdot)||^2_{L^2(\Omega)}\,dt \leq C(T)||u_0||^2_{L^2(\Omega)}$$

Proof. The proof follows the same lines as the previous Theorem 3.2.
Thanks to (2.2) $\mathcal{B}^d(u_h, q_h, v_h; \varphi_u, \varphi_q, \varphi_v) = 0$ for all $\varphi_u, \varphi_q, \varphi_v \in V^k$, then in particular we have $\mathcal{B}^d(u_h, q_h, v_h; u_h, v_h, -q_h) = 0$.

From Lemma 3.1 we have

$$\begin{aligned}
\frac{1}{2}||u_h(T,\cdot)||^2_{L^2(\Omega)} - \frac{1}{2}||u_0||^2_{L^2(\Omega)} + \int_0^T ||v_h(t,\cdot)||^2_{L^2(\Omega)}\,dt - \int_0^T (\mathcal{J}_1^d[v_h], v_h)\,dt \\
- \int_0^T (\mathcal{J}_2^d[u_h], v_h)\,dt + \int_0^T \sum_{j=1}^M \left([\Phi(u_h)]_j - (\hat{f}_h[u_h])_j\right)\,dt = 0
\end{aligned}$$

Thanks to the monotone property of the flux $\hat{f}_h$ (i.e. increasing w.r.t its first variable and decreasing w.r.t the second variable) we have

$$\int_{u_j^-}^{u_j^+} \left(f(x) - \hat{f}_h(u_j^-, u_j^+)\right)dx \geq 0,$$

using now a change of variable we get

$$\int_{u_j^-}^{u_j^+} \Big(f(x) - \hat{f}_h(u_j^-, u_j^+) \Big)\, dx = [\Phi(u)]_j - (\hat{f}_h[u])_j$$

and then we have $[\Phi(u_h)]_j - (\hat{f}_h[u_h])_j > 0$.
Therefore we obtain

$$\frac{1}{2}||u_h(T,\cdot)||^2_{L^2(\Omega)} - \frac{1}{2}||u_0||^2_{L^2(\Omega)} + \int_0^T ||v_h(t,\cdot)||^2_{L^2(\Omega)}\, dt - \int_0^T (\mathcal{J}_1^d[v_h], v_h)\, dt - \int_0^T (\mathcal{J}_2^d[u_h], v_h)\, dt \leq 0$$

We finally conclude the proof by using Lemma 2.1, Hölder's inequality and Gronwall's Lemma. □

4. Errors estimates

We consider the following special projections $\mathcal{P}^{\pm}$ and $\mathcal{Q}$ into V^k :
For all intervals $I_j, j = 0, \cdots, M$

$$\int_{I_j} (\mathcal{P}^{\pm}u(x) - u(x))v(x)\, dx = 0, \quad \forall v \in P^{k-1}(I_j)$$
$$\mathcal{P}^- u(x_j) = u(x_j^-), \qquad \mathcal{P}^+ u(x_j) = u(x_j^+).$$

and $\mathcal{Q}$ is the standard L^2 projection defined as

$$\int_{I_j} (\mathcal{Q}u(x) - u(x))v(x)\, dx = 0, \quad \forall v \in P^k(I_j)$$

Lemma 4.1. *The following result holds*

(1) *Signal Model.*

$$\begin{aligned} & \mathcal{B}^s(\mathcal{P}^- u - u, \mathcal{P}^+ q - q, \mathcal{Q}v - v; \mathcal{P}^- e_u, \mathcal{Q}e_v, -\mathcal{P}^+ e_q) \\ = & \int_0^T \sum_{j=0}^M ((\mathcal{P}^- u - u)_t, \mathcal{P}^- e_u)_{I_j}\, dt + \int_0^T \sum_{j=0}^M (\mathcal{P}^+ q - q, \mathcal{Q}e_v)_{I_j}\, dt \\ - & \int_0^T \sum_{j=0}^M (\mathcal{J}_1^s[\mathcal{Q}v - v], \mathcal{Q}e_v)_{I_j}\, dt - \int_0^T \sum_{j=0}^M (\mathcal{J}_2^s[\mathcal{P}^- u - u], \mathcal{Q}e_v)_{I_j}\, dt \end{aligned}$$

(2) *Dune Model.*

$$\begin{aligned} & \mathcal{B}_l^d(\mathcal{P}^- u - u, \mathcal{P}^+ q - q, \mathcal{Q}v - v; \mathcal{P}^- e_u, \mathcal{Q}e_v, -\mathcal{P}^+ e_q) \\ = & \int_0^T \sum_{j=0}^M ((\mathcal{P}^- u - u)_t, \mathcal{P}^- e_u)_{I_j} dt + \int_0^T \sum_{j=0}^M (\mathcal{P}^+ q - q, \mathcal{Q}e_v)_{I_j}\, dt \\ - & \int_0^T \sum_{j=0}^M (\mathcal{J}_1^d[\mathcal{Q}v - v], \mathcal{Q}e_v)_{I_j}\, dt - \int_0^T \sum_{j=0}^M (\mathcal{J}_2^d[\mathcal{P}^- u - u], \mathcal{Q}e_v)_{I_j}\, dt \end{aligned}$$

Proof. (1) Signal Model.

From (3.3) we have

$$\begin{aligned}
&\mathcal{B}^s(\mathcal{P}^-u-u,\mathcal{P}^+q-q,\mathcal{Q}v-v;\mathcal{P}^-e_u,\mathcal{Q}e_v,-\mathcal{P}^+e_q)\\
=&\int_0^T\sum_{j=0}^M((\mathcal{P}^-u-u)_t,\mathcal{P}^-e_u)_{I_j}\,dt-\int_0^T\sum_{j=0}^M(\mathcal{P}^+q-q,(\mathcal{P}^-e_u)_x)_{I_j}dt\\
-&\int_0^T\sum_{j=1}^M(\widehat{\mathcal{P}^+q-q})_j[\mathcal{P}^-e_u]_j\\
-&\int_0^T\left((\mathcal{P}^+q(-1,t)-q(-1,t))^+P^-e_u(-1,t)-(\mathcal{P}^+q(1,t)-q(1,t))^-\mathcal{P}^-e_u(1,t)\right)\,dt\\
+&\int_0^T\sum_{j=0}^M(\mathcal{P}^+q-q,\mathcal{Q}e_v)_{I_j}\,dt+\int_0^T\sum_{j=0}^M(\mathcal{Q}v-v,\mathcal{Q}e_v)_{I_j}\,dt-\int_0^T\sum_{j=0}^M(\mathcal{J}_1^s[\mathcal{Q}v-v],\mathcal{Q}e_v)_{I_j}\,dt\\
-&\int_0^T\sum_{j=0}^M(\mathcal{J}_2^s[\mathcal{P}^-u-u],\mathcal{Q}e_v)_{I_j}\,dt-\int_0^T\sum_{j=0}^M(\mathcal{Q}v-v,\mathcal{P}^+e_q)_{I_j}\,dt\\
-&\int_0^T\sum_{j=0}^M(\mathcal{P}^-u-u,(\mathcal{P}^+e_q)_x)_{I_j}\,dt-\int_0^T\sum_{j=1}^M(\widehat{\mathcal{P}^-u-u})_j[\mathcal{P}^+e_q]_j\,dt
\end{aligned}$$

Using the properties of the projection $\mathcal{P}^\pm,\mathcal{Q}$, we have

$$\begin{aligned}
(\mathcal{P}^+q-q,(\mathcal{P}^-e_u)_x)_{I_j}=0,\quad(\mathcal{Q}v-v,\mathcal{Q}e_v)_{I_j}=0,\\
(\mathcal{Q}v-v,\mathcal{P}^+e_q)_{I_j}=0,\quad(\mathcal{P}^-u-u,(\mathcal{P}^+e_q)_x)_{I_j}=0\\
(\widehat{\mathcal{P}^-u-u})_j=0,\quad(\widehat{\mathcal{P}^+q-q})_j=0
\end{aligned}$$

We then obtain

$$\begin{aligned}
&\mathcal{B}^s(\mathcal{P}^-u-u,\mathcal{P}^+q-q,\mathcal{Q}v-v;\mathcal{P}^-e_u,\mathcal{Q}e_v,-\mathcal{P}^+e_q)\\
=&\int_0^T\sum_{j=0}^M((\mathcal{P}^-u-u)_t,\mathcal{P}^-e_u)_{I_j}\,dt+\int_0^T\sum_{j=0}^M(\mathcal{P}^+q-q,\mathcal{Q}e_v)_{I_j}\,dt\\
-&\int_0^T\sum_{j=0}^M(\mathcal{J}_1^s[\mathcal{Q}v-v],\mathcal{Q}e_v)_{I_j}\,dt-\int_0^T\sum_{j=0}^M(\mathcal{J}_2^s[\mathcal{P}^-u-u],\mathcal{Q}e_v)_{I_j}\,dt
\end{aligned}$$

(2) Dune Model. The proof is similar to the previous ones.

□

We are now ready to prove the error estimates of our numerical schemes.

4.1. **Error estimate for the signal model.**

Theorem 4.2. *Let u be the sufficiently smooth exact solution to* (1.4) *and let $u_h\in C^1([0,T];V^k)$ be the numerical solution of* (2.1). *Then, with $e_h:=u-u_h$ there holds the following error estimate:*

$$||e_h(T,\cdot)||\le C\Delta x^{k+1}||\partial_x^{k+1}u(T,\cdot)||, \tag{4.1}$$

where $C = C(k, \lambda, T)$ is a constant depending on k, λ and T but independent of u and Δx.

Proof. We denote

$$e_u = u - u_h,\ e_q = q - q_h \text{ and } e_v = v - v_h.$$

We then recover the error equation:

$$\mathcal{B}^s(e_u, e_q, e_v; \varphi_u, \varphi_q, \varphi_v) = 0, \quad \forall \varphi_u, \varphi_q, \varphi_v \in V^k$$

We obtain after rearranging terms,

$$\mathcal{B}^s(u^e, q^e, v^e; \varphi_u, \varphi_q, \varphi_v) = \mathcal{B}^s(\mathcal{P}^- u - u, \mathcal{P}^+ q - q, \mathcal{Q}v - v; \varphi_u, \varphi_q, \varphi_v), \quad \forall \varphi_u, \varphi_q, \varphi_v \in V^k.$$

where $u^e = \mathcal{P}^- u - u_h, q^e = \mathcal{P}^+ q - q_h$ and $v^e = \mathcal{Q}v - v_h$,
and for $\varphi_u = u^e, \varphi_q = v^e, \varphi_v = -q^e$ we obtain

$$\mathcal{B}^s(u^e, q^e, v^e; u^e, v^e, -q^e) = \mathcal{B}^s(\mathcal{P}^- u - u, \mathcal{P}^+ q - q, \mathcal{Q}v - v; u^e, v^e, -q^e).$$

From Lemma 3.1, we have

$$\begin{aligned}\mathcal{B}^s(u^e, q^e, v^e; u^e, v^e, -q^e) &= \int_0^T \frac{1}{2}\frac{d}{dt}||u^e(t)||^2_{L^2(\Omega)}\, dt + \int_0^T \sum_{j=0}^{M} ||v(t)^e||^2_{L^2(I_j)}\, dt \\ &\quad - \int_0^T \sum_{j=0}^{M} (\mathcal{J}_1^s[v^e], v^e)_{I_j}\, dt - \int_0^T \sum_{j=0}^{M} (\mathcal{J}_2^s[u^e], v^e)_{I_j}\, dt.\end{aligned}$$

and from Lemma 4.1

$$\begin{aligned}\mathcal{B}^s(\mathcal{P}^- u - u, \mathcal{P}^+ q - q, \mathcal{Q}v - v; u^e, v^e, -q^e) &= \int_0^T \left((\mathcal{P}^- u - u)_t, u^e\right)\, dt \\ + \int_0^T \sum_{j=0}^{M} (\mathcal{P}^+ q - q, v^e)_{I_j}\, dt &- \int_0^T \sum_{j=0}^{M} (\mathcal{J}_1^s[\mathcal{Q}v - v], v^e)_{I_j}\, dt \\ - \int_0^T \sum_{j=0}^{M} (\mathcal{J}_2^s[\mathcal{P}^- u - u], v^e)_{I_j}\, dt &\end{aligned}$$

Therefore, we have

$$\begin{aligned}&\int_0^T \frac{1}{2}\frac{d}{dt}||u^e(t)||^2_{L^2(\Omega)} + \int_0^T \sum_{j=0}^{M} ||v^e(t)||^2_{L^2(I_j)} - \int_0^T \sum_{j=0}^{M} (\mathcal{J}_1^s[v^e], v^e)_{I_j} - \int_0^T \sum_{j=0}^{M} (\mathcal{J}_2^s[u^e], v^e)_{I_j}\, dt \\ = &\int_0^T (\mathcal{P}^- u - u)_t, u^e)\, dt + \int_0^T \sum_{j=0}^{M} (\mathcal{P}^+ q - q, v^e)_{I_j}\, dt \\ - &\int_0^T \sum_{j=0}^{M} (\mathcal{J}_1^s[\mathcal{Q}v - v], v^e)_{I_j}\, dt - \int_0^T \sum_{j=0}^{M} (\mathcal{J}_2^s[\mathcal{P}^- u - u], v^e)_{I_j}\, dt \\ &\qquad (4.2)\end{aligned}$$

Then using Lemma 2.1, the error associated with the projection operators [29], Cauchy-Schwartz, Holder inequalities and the initial error $||u_0^e|| = 0$ (obtained thanks to the last equation of system (2.1)), (4.2) gives

$$\frac{1}{2}||u^e(T)||^2_{L^2(\Omega)} + \int_0^T \sum_{j=0}^{M} ||v^e(t)||^2_{L^2(I_j)}\,dt \le C_*(r^{\frac{\lambda}{2}}) \int_0^T \sum_{j=0}^{M} ||v^e(t)||^2_{L^2(I_j)}\,dt$$
$$+4\int_0^T \sum_{j=0}^{M} ||\mathcal{J}_2^s[u^e]||^2_{L^2(I_j)}\,dt + \frac{1}{16}\int_0^T \sum_{j=0}^{M} ||v^e||^2_{L^2(I_j)} + \int_0^T (\mathcal{P}^- u - u)_t, u^e)\,dt$$
$$+4\int_0^T \sum_{j=0}^{M} ||\mathcal{P}^+ q - q||^2_{L^2(I_j)} + \frac{1}{16}\int_0^T \sum_{j=0}^{M} ||v^e||^2_{L^2(I_j)} + 4\sum_{j=0}^{M}\int_0^T ||\mathcal{J}_1^s[\mathcal{Q}v - v]||^2_{L^2(I_j)}$$
$$+\frac{1}{16}\int_0^T \sum_{j=0}^{M} ||v^e||^2_{L^2(I_j)} + 4\int_0^T \sum_{j=0}^{M} ||\mathcal{J}_2^s[\mathcal{P}^- u - u]||^2_{L^2(I_j)} + \frac{1}{16}\int_0^T \sum_{j=0}^{M} ||v^e||^2_{L^2(I_j)} \le$$
$$\int_0^T \left(C_*(r^{\lambda/2}) \sum_j ||v^e||^2_{L^2(I_j)} + \frac{1}{4}\sum_{j=0}^{M} ||v^e||^2_{L^2(I_j)} + C(r^\lambda)\Delta x^{2(k+1)}|u|^2_{k+2} \right) dt$$
$$+\int_0^T \left(C(r^{-2\lambda})\Delta x^{2(k+1)}|u|^2_{k+1} + C(r^{-2\lambda})||u^e||^2_{L^2(I_j)} \right) dt$$

and if we choose r such that $C_*(r^{\lambda/2}) = \frac{1}{4}$, we obtain

$$\frac{1}{2}||u^e(T)||^2_{L^2(\Omega)} + \frac{1}{2}\int_0^T \sum_{j=0}^{M} ||v^e(t)||^2_{L^2(I_j)} \le \int_0^T \left(C(\lambda, |u|_{k+1}, |u|_{k+2})\Delta x^{2(k+1)} + C(\lambda)||u^e||^2_{L^2(\Omega)} \right) dt$$

Finally, using Gronwall's Lemma we get

$$||u^e(T)||^2_{L^2(\Omega)} + \int_0^T \sum_{j=0}^{M} ||v^e(t)||^2_{L^2(I_j)}\,dt \le C(k, \lambda, T, |u|_{k+1}, |u|_{k+2})\Delta x^{2k+2}$$

□

4.2. **Error estimate for the dune model.**

4.2.1. *The linear case $f = c\,u$.* In this subsection we consider the linear problem

$$\begin{cases} u_t + \big(cu - u_x + \mathcal{J}^d[u_x]\big)_x = 0, \\ u(0,x) = u_0(x). \end{cases} \tag{4.3}$$

For the convection term, we opt for the well-known monotone Lax-Friedrich flux [12]

$$\hat{f}(u_i^-, u_i^+) = c\overline{u_i} - |c|\frac{[u]_i}{2}. \tag{4.4}$$

Theorem 4.3. *Let u be the sufficiently smooth exact solution to (4.3) and $u_h \in C^1([0,T]; V^k)$ be a solution of (2.2) with $f(u) = c\,u$ and the numerical flux (4.4) . With $e_u := u - u_h$, we have the following error estimate:*

$$||e_h(T,\cdot)|| \le C\Delta x^{k+1}||\partial_x^{k+1}u(T,\cdot)||, \tag{4.5}$$

where $C = C(k, c, T)$ is a constant depending on c, k and T but independent of u and Δx.

Proof. The proof follows the same lines as the previous Theorem 4.2. The difference here resides on the presence of the convection term.
As previously, we have

$$\mathcal{B}^d(u^e,q^e,v^e;u^e,v^e,-q^e)=\mathcal{B}^d(\mathcal{P}^-u-u,\mathcal{P}^+q-q,\mathcal{Q}v-v;u^e,v^e,-q^e),$$

where $u^e=\mathcal{P}^-u-u_h, q^e=\mathcal{P}^+q-q_h$ and $v^e=\mathcal{Q}v-v_h$. From Lemma 3.1, we have

$$\begin{aligned}\mathcal{B}^d(u^e,q^e,v^e;u^e,v^e,-q^e)&=\frac{1}{2}||u^e(T)||^2_{L^2(\Omega)}+\int_0^T\sum_{j=0}^M||v^e(t)||^2_{L^2(I_j)}\\&-\int_0^T\sum_{j=0}^M(\mathcal{J}_1^d[v^e],v^e)_{I_j}-\int_0^T\sum_{j=0}^M(\mathcal{J}_2^d[u^e],v^e)_{I_j}\\&-\int_0^T\sum_{j=0}^M(cu^e,(u^e)_x)_{I_j}-\int_0^T\sum_{j=0}^M(c\overline{(u^e)}_j-\frac{|c|}{2}[u^e]_j)[u^e]_j\\&=\frac{1}{2}||u^e(T)||^2_{L^2(\Omega)}+\int_0^T\sum_{j=0}^M||v^e(t)||^2_{L^2(I_j)}-\int_0^T\sum_{j=0}^M(\mathcal{J}_1^d[v^e],v^e)_{I_j}\\&-\int_0^T\sum_{j=0}^M(\mathcal{J}_2^d[u^e],v^e)_{I_j}+\int_0^T\sum_{j=0}^M\frac{|c|}{2}[u^e]_j^2\end{aligned}\tag{4.6}$$

Moreover, from Lemma 4.1, we obtain

$$\begin{aligned}&\mathcal{B}^d(\mathcal{P}^-u-u,\mathcal{P}^+q-q,\mathcal{Q}v-v;u^e,v^e,-q^e)=\int_0^T((\mathcal{P}^-u-u)_t,u^e)dt\\&+\int_0^T\sum_{j=0}^M(\mathcal{P}^+q-q,v^e)_{I_j}-\int_0^T\sum_{j=0}^M(\mathcal{J}_1^d[\mathcal{Q}v-v],v^e)_{I_j}\,dt-\int_0^T\sum_{j=0}^M(\mathcal{J}_2^d[\mathcal{P}^-u-u],v^e)_{I_j}\,dt\end{aligned}\tag{4.7}$$

Finally, as the proof of Theorem 4.2, by using (4.6), (4.7), Lemma 2.1, the error associated to the projections operators [29] and Gronwall's Lemma, we obtain for r well chosen

$$||u^e(T)||^2_{L^2(\Omega)}+\int_0^T\sum_{j=0}^M||v^e(t)||^2_{L^2(I_j)}dt+\int_0^T\sum_{j=0}^M\frac{|c|}{2}[u^e]_j^2dt\leq C(k,T,|u|_{k+1},|u|_{k+2})\,\Delta x^{2k+2}$$

□

4.2.2. *The nonlinear case.* To deal with the nonlinearity we argue as [29] and we use the following results:

Lemma 4.4 ([31])**.** *For any piecewise smooth function $w\in L^2(\Omega)$, on each cell boundary point we define*

$$\kappa(\hat{f};w)\equiv\kappa(\hat{f};w^-,w^+):=\begin{cases}[w]^{-1}(f(\overline{w})-\hat{f}(w)) & \text{if } [w]\neq 0\\ \frac{1}{2}|f'(\overline{w})| & \text{if } [w]=0,\end{cases}$$

where $\hat{f}(w)\equiv\hat{f}(w^-,w^+)$ is a monotone numerical flux consistent with the given flux f. Then $\kappa(\hat{f};w)$ is nonnegative and bounded for any $(w^-,w^+)\in\mathbb{R}$. Moreover,

we have

$$\frac{1}{2}|f'(\overline{w})| \leq \kappa(\hat{f};w) + C_*|[w]|,$$
$$-\frac{1}{8}f''(\overline{w})[w] \leq \kappa(\hat{f};w) + C_*|[w]|^2.$$

To estimate the nonlinear part, we define as in [28]

$$\sum_{j=0}^{M}\mathcal{H}_j(f;u,u_h,v) = \sum_{j=0}^{M}\int_{I_j}(f(u)-f(u_h))v_x\,dx + \sum_{j=0}^{M}((f(u)-f(\overline{u}_h))[v])_j + \sum_{j=0}^{M}((f(\overline{u}_h)-\hat{f})[v])_j$$

Lemma 4.5 ([28])**.** *For $\mathcal{H}_j(f;u,u_h,v)$ defined above, we have the following estimate:*

$$\begin{aligned}\sum_{j=0}^{M}\mathcal{H}_j(f;u,u_h,v) &\leq -\frac{1}{4}\kappa(\hat{f};u_h)[v]^2 + (C + C_\star(||v||_\infty + \Delta x^{-1}||e_u||_\infty^2))||v||_{L^2(\Omega)}^2 \\ &+ (C + C_\star\Delta x^{-1}||e_u||_\infty^2)\Delta x^{2k+1}\end{aligned}$$

As in [28] we consider for Δx small and $k \geq 1$ the following assumption

$$||u - u_h|| \leq \Delta x. \tag{4.8}$$

Theorem 4.6. *Let u be the sufficiently smooth exact solution to* (1.2) *and $u_h \in C^1([0,T];V^k)$ be the discrete solution of the LDG scheme* (2.2)*. We have for Δx small enough satisfying* (4.8) *and $k \geq 1$,*

$$||u - u_h|| \leq C\Delta x^{k+\frac{1}{2}}.$$

Proof. Using previous notations, (2.2) and by adding $\pm\int_0^T\sum_{j=0}^{M}(f(\overline{u}_h)[\varphi_u])_j$, we have for any $\varphi_u,\varphi_q,\varphi_v \in V^k$

$$\begin{aligned}&\mathcal{B}^d(u,q,v;\varphi_u,\varphi_q,\varphi_v) - \mathcal{B}^d(u_h,q_h,v_h;\varphi_u,\varphi_q,\varphi_v)\\ &:= \mathcal{B}_l^d(u,q,v;\varphi_u,\varphi_q,\varphi_v) - \mathcal{B}_l^d(u_h,q_h,v_h;\varphi_u,\varphi_q,\varphi_v) - \int_0^T\sum_{j=0}^{M}(f(u),\varphi_u')\,dt\\ &- \int_0^T\sum_{j=0}^{M}(f(u)[\varphi_u])_j\,dt + \int_0^T\sum_{j=0}^{M}(f(u_h),\varphi_u')_{I_j}\,dt + \int_0^T\sum_{j=0}^{M}\left(\hat{f}[\varphi_u]\right)_j\,dt\\ &= \mathcal{B}_l^d(u-u_h,q-q_h,v-v_h;\varphi_u,\varphi_q,\varphi_v) - \int_0^T\sum_{j=0}^{M}(f(u)-f(u_h),\varphi_u')_{I_j}\,dt\\ &- \int_0^T\sum_{j=0}^{M}((f(u)-f(\overline{u}_h))[\varphi_u])_j\,dt - \int_0^T\sum_{j=0}^{M}\left((f(\overline{u}_h)-\hat{f})[\varphi_u]\right)_j\,dt\\ &= \mathcal{B}_l^d(u-u_h,q-q_h,v-v_h;\varphi_u,\varphi_q,\varphi_v) - \int_0^T\sum_{j=0}^{M}\mathcal{H}_j(f;u,u_h,\varphi_u)\,dt\\ &= 0\end{aligned}$$

Setting $(\varphi_u, \varphi_q, \varphi_v) = (u^e, v^e, -q^e)$ we obtain

$$\begin{aligned}\mathcal{B}_l^d(u^e, q^e, v^e; u^e, v^e, -q^e) &= \mathcal{B}_l^d(\mathcal{P}^- u - u, \mathcal{P}^+ q - q, \mathcal{Q}v - v; u^e, v^e, -q^e) \\ &+ \int_0^T \sum_{j=0}^M \mathcal{H}_j(f; u, u_h, u^e)\end{aligned}$$

Using Lemma 3.1, Lemma 4.1 and Lemma 4.5, we obtain

$$\begin{aligned}&||u^e(T)||^2_{L^2(\Omega)} + \int_0^T \sum_{j=0}^M ||v^e(t)||^2_{L^2(I_j)}\, dt - \int_0^T \sum_{j=0}^M (\mathcal{J}_1^d[v^e], v^e)_{I_j}\, dt \\ &- \int_0^T \sum_{j=0}^M (\mathcal{J}_2^d[u^e], v^e)_{I_j}\, dt + \frac{1}{4}\kappa(\hat{f}; u)[u^e]^2 \\ &\leq \int_0^T ((\mathcal{P}^- u - u)_t, u^e)\, dt + \int_0^T \sum_{j=0}^M (\mathcal{P}^+ q - q, v^e)_{I_j}\, dt \\ &- \int_0^T \sum_{j=0}^M (\mathcal{J}_1^d[\mathcal{Q}v - v], v^e)_{I_j}\, dt - \int_0^T \sum_{j=0}^M (\mathcal{J}_2^d[\mathcal{P}^- u - u], v^e)_{I_j}\, dt \\ &+ \int_0^T (C + C_\star(||u^e||_\infty + \Delta x^{-1}||e_u||^2_\infty))||u^e||^2_{L^2(\Omega)} + (C + C_\star \Delta x^{-1}||e_u||^2_\infty)\Delta x^{2k+1}\, dt\end{aligned}$$

The terms from the linear parts are analyzed in the same way as the proof of Theorem 4.2. We control these terms using Lemma 2.1 and error properties for the projection operators [29]. Again the paramater r is chosen in a way that we can control the operator $\mathcal{J}_1^d$ with the diffusive term. For the nonlinear part, we consider Lemma 4.5 and the assumption (4.8) to control the nonlinear terms. We finally conclude the proof by applying the Gronwall's Lemma.

□

5. Numerical simulations

We conclude this paper by presenting some experimental results obtained using the local discontinuous Galerkin method (see numerical schemes (2.2) and (2.1)) with different polynomial order for the space discretization, an Euler explicit method for the time discretization and we take $r = 0.2$.

Test 1: Numerical convergence To study the numerical convergence we consider

$$u_t - u_{xx} + \partial_x(\mathcal{J}_1^d[u_x] + \mathcal{J}_2^d[u]) = 0, \qquad \Omega = (-1, 1) \tag{5.1}$$

with the following two initial data

Test 1a: $u(0, x) = e^{-50(x+0.2)^2}$,

Test 1b: $u(0, x) = e^{-50(x+0.4)^2} + e^{-50(x-0.4)^2}$.

We compute the numerical solution of this problem at time $T = 0.1$. LDG methods based on P^k polynomial approximations with $k = 1, 2$ are tested.

Table 1, Figure 1 and Figure 2 display the convergence numerical order for both

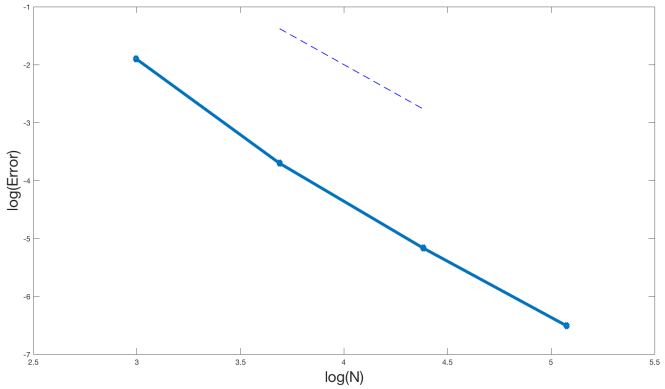

FIGURE 1. Test 1a: Convergence curve (solid line) for one order polynomial approximations ($k = 1$). Dashed line represents a slope of order two. N denotes the number of elements.

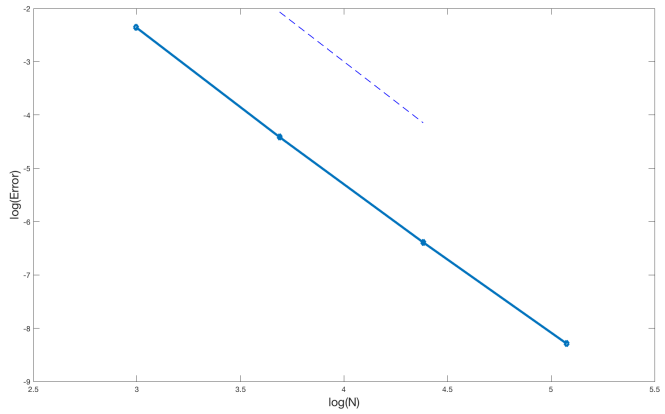

FIGURE 2. Test 1b: Convergence curve (solid line) for second order polynomial approximations ($k = 2$). Dashed line represents a slope of order three. N denotes the number of elements.

examples. In Figures 1 and 2 we plot the logarithm of the error (in norm L^2) in function of the logarithm of the number of elements N. The time step is chosen in a way that the condition $\Delta t = \beta \Delta x^2$ with $\beta < 0.5$ is satisfied. The convergence numerical order is then given by the slope of this curve. For reference, a small line (the dashed line) of slope two and three are added in the figures. We observe that the numerical rate of convergence is slightly better approximation than two when P^1 is considered and it is approaching three when P^2 is considered.

N	error ($k=1$)	order	error ($k=2$)	order
40	0.1510	-	0.09520	-
80	0.0247	2.6112	0.0121	2.9760
160	0.0057	2.1157	0.00168	2.8485
320	0.0014	2.0255	0.000251	2.7427

TABLE 1. Test 1: Error and numerical rate of convergence for one order polynomial approximations ($k = 1$) and for second order polynomial approximations ($k = 2$). N denotes the number of elements.

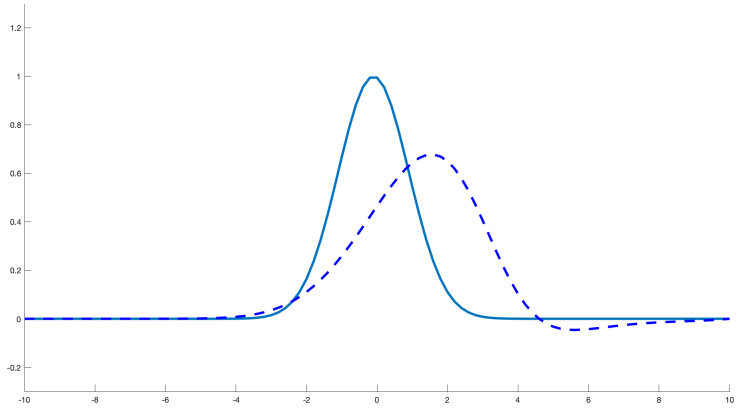

FIGURE 3. Test 2: Piecewise linear (P^1) approximations with $N = 100$. Solid line: initial data, dashed line: numerical solution at $T = 1$.

Test 2: Dune model. In this example, we simulate using P^1 approximations the nonlinear dune model

$$\begin{aligned} u_t - u_{xx} + uu_x + \partial_x(\mathcal{J}_1^d[u_x] + \mathcal{J}_2^d[u]) &= 0, \quad x \in \Omega = (-10, 10), \quad t \in (0, T), \\ u(0, x) &= e^{-0.5(x+0.1)^2} \end{aligned} \tag{5.2}$$

The numerical result is presented in Figure 3: the solid line represents the initial data and the dashed line the numerical solution at the time $T = 1$. In this simulation, we take $\Delta x = 0.2$ and $\Delta t = 0.016$.
As we expect from the linearized viscous Burger equation, the initial data is propagated downstream but we can see here in addition an erosive process due to the nonlocal term.

Test 3: Signal filtering model. In this example, we consider the following signal filtering equation

$$u_t - \varepsilon\, u_{xx} + \eta\, \partial_x(\mathcal{J}_1^s[u_x] + \mathcal{J}_2^s[u]) = 0$$

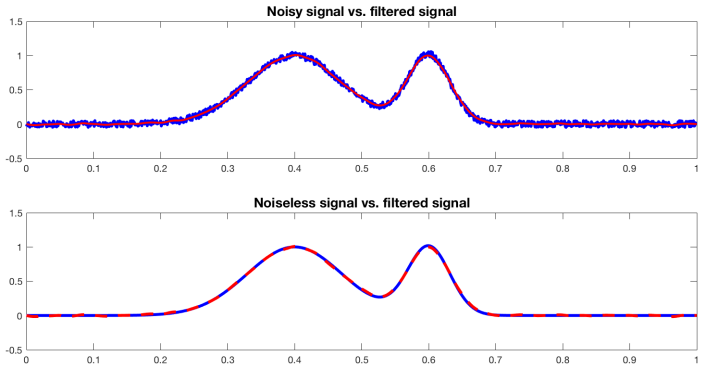

FIGURE 4. Test 3: Top : noisy signal (bleu) vs. filtered signal (red) ; Bottom: noiseless signal (blue line) vs. filtered signal (dashed red line) using P^1 approximations.

with $\alpha = 1.5$ and we consider as initial data two Gaussians corrupted by a random noise $n(x)$

$$u(0,x) = e^{-100(x-2/5)^2} + e^{-500(x-3/5)^2} + n(x)$$

Figure 4 illustrates filtered signal for $T = 1, \varepsilon = 10$, $\eta = 1$ and N = 100. As we can see, the noise is very well eliminated and we find again the original signal. The difference with the heat equation is that the shape of the signal is preserved thanks to the anti-diffusive fractional operator.

REFERENCES

[1] Aboelenen, T and El-Hawary, H.M., *A high-order nodal discontinuous Galerkin method for a linearized fractional Cahn-Hilliard equation*, Computers & Mathematics with Applications (73), 2017

[2] Ahmadinia, M., Safari, Z. Fouladi, S., *Analysis of local discontinuous Galerkin method for time–space fractional convection–diffusion equations* , BIT Numerical Mathematics, 2018

[3] Alibaud, N. and Azerad, P. and Isèbe, D., *A non-monotone nonlocal conservation law for dune morphodynamics*, Differential and Integral Equations. An International Journal for Theory & Applications (23), 2010

[4] Azerad P., Bouharguane A. and Crouzet J.-F., *Simultaneous denoising and enhancement of signals by a fractal conservation law* , Communications in Nonlinear Science and Numerical Simulation (17), 2012.

[5] Betancourt F., Burger R., Karlsen K H and Tory E M , *On nonlocal conservation laws modelling sedimentation*, Nonlinearity (24), 2011

[6] Blandin S. and Goatin P. , *Well-posedness of a conservation law with non-local flux arising in traffic flow modeling* Numerische Mathematik (132), 2016

[7] Bouharguane A. and Carles R., *Splitting methods for the nonlocal Fowler equation*, Mathematics of Computation (83), 2014.

[8] Bouharguane A., *Finite element method for a space-fractional anti-diffusive equation*, Journal of Computational and Applied Mathematics, 2017

[9] Bueno-Orovio A., Kay D., Burrage K., *Fourier spectral methods for fractional-in-space reaction-diffusion equations* , BIT numerical mathematics (54), 2014

[10] Cifani S., Jakobsen E R and Karlsen K H, *The discontinuous Galerkin method for fractional degenerate convection-diffusion equations*, BIT Numerical Mathematics (51), 2011

[11] Cockburn B. and Shu C.-W., *The Local Discontinuous Galerkin Method for Time-Dependent Convection-Diffusion Systems*, SIAM Journal on Numerical Analysis (35), 1998

[12] Cockburn B. and Shu, C.-W., *Runge–Kutta Discontinuous Galerkin Methods for Convection-Dominated Problems*, Journal of Scientific Computing (16), 2001

[13] Cockburn B. and Mustapha K., *A hybridizable discontinuous Galerkin method for fractional diffusion problems*, Numerische Mathematik (130), 2015.

[14] Deng W., *Finite Element Method for the Space and Time Fractional FokkerPlanck Equation*, SIAM Journal on Numerical Analysis (47), 2009

[15] Deng, W.H. and Hesthaven, J.S., *Local Discontinuous Galerkin methods for fractional diffusion equations*, ESAIM: M2AN (47), 2013

[16] Droniou J., *A numerical method for fractal conservation laws*, Mathematics of Computation (79), 2010

[17] Fowler, A. C., *Dunes and drumlins*, Geomorphological fluid mechanics (211), 2001

[18] Kouakou, K. K.J. and Lagre, P.-Y., *Stability of an erodible bed in various shear flows*, The European Physical Journal B - Condensed Matter and Complex Systems (47), 2005.

[19] Li, Can and Zhao, Shan, *Efficient Numerical Schemes for Fractional Water Wave Models*, Comput. Math. Appl. (71), 2016

[20] Li M., Huang C. and Wang N., *Galerkin finite element method for the nonlinear fractional Ginzburg-Landau equation*, Applied Numerical Mathematics (118), 2017

[21] Liu H. and Yan J., *The direct discontinuous Galerkin (DDG) method for diffusion with interface corrections*, Communications in Computational Physics (8), 2010

[22] Matache A., Schwab C. and Wihler T., *Fast Numerical Solution of Parabolic Integrodifferential Equations with Applications in Finance*, SIAM Journal on Scientific Computing (27), 2005

[23] Meerschaert M. and Tadjeran C., *Finite difference approximations for fractional advection-dispersion flow equations*, Journal of Computational and Applied Mathematics (172), 2004

[24] Mustapha K. and McLean W., *Superconvergence of a Discontinuous Galerkin Method for Fractional Diffusion and Wave Equations*, SIAM Journal on Numerical Analysis (51), 2013

[25] Safari F. and Chen W., *Coupling of the improved singular boundary method and dual reciprocity method for multi-term time-fractional mixed diffusion-wave equations*, Computers & Mathematics with Applications, 2019

[26] Shen J.,*On a new pseudocompressibility method for the incompressible Navier-Stokes equations*, Applied Numerical Mathematics (21), 1996

[27] Vong S. and Luy P., *On a second order scheme for space fractional diffusion equations with variable coefficients* , Applied Numerical Mathematics (137), 2019

[28] Xu Y. and Shu C.-W., *Error estimates of the semi-discrete local discontinuous Galerkin method for nonlinear convection didiffusion and KdV equations*, Computer Methods in Applied Mechanics and Engineering (196), 2007

[29] Xu Q. and Hesthaven J. S., *Discontinuous Galerkin method for fractional convection-diffusion equations*, SIAM Journal on Numerical Analysis (52), 2014

[30] Yan J. and Shu C.-W., *Local Discontinuous Galerkin Methods for Partial Differential Equations with Higher Order Derivatives*, Journal of Scientific Computing (17), 2002

[31] Zhang Q. and Shu C.-W., *Error Estimates to Smooth Solutions of Runge–Kutta Discontinuous Galerkin Methods for Scalar Conservation Laws*, SIAM Journal on Numerical Analysis (42), 2004

[32] Zheng Y., Li C. and Zhao Z., *A Note on the Finite Element Method for the Space-fractional Advection Diffusion Equation*, Computers & Mathematics with Applications (59), 2010